Molecularly Imprinted Electrochemical Sensor for Determination of Tetrahydrocannabinol in Human Blood Plasma

Yi Zhao[1], Youngchul Moon[1,], Rojan Savari[2,*]*

[1] School of College of Art and Physical Education, Hanyang University; Seoul 04763 Korea
[2] School of Physics, College of Science, University of Tehran, North-Kargar Street, Tehran, 1439955961, Iran
[*]E-mail: moonyoungchul166@sohu.com

The goal of this study was to create a molecular imprinting-based sensor on MWCNTs modified electrode for the selective determination of Δ^9-tetrahydrocannabinol (Δ^9-THC) as doping agent in biological fluids samples of athletes. as a doping agent in athlete biological fluid samples. The MWCNTs nanostructures were electrodeposited on the screen printed carbon electrode (MWCNTs/SPCE), and MIP was electropolymerized on the MWCNTs/SPCE surface (MIP/MWCNTs/SPCE). SEM and XRD analyses revealed that a thin layer of MIP particles covered MWCNTs without changing their morphology. Electrochemical studies using CV and DPV measurements revealed that MIP/MWCNTs nanostructured electrodes significantly improved electrocatalytic activity and electivity. Results demonstrated that the minimal detectable limit for Δ^9-THC was 0.37 ng/mL (S/N=3), the sensitivity of MIP/MWCNTs/SPCE THC was obtained at 0.00155 μA/ng.mL^{-1}, and linearity was over a concentration range of 0-3150 ng/mL with correlation coefficients of the standard curves > 0.99. The applicability and validity of MIP/MWCNTs/SPCE were investigated for Δ^9-THC determination level in a cyclist's blood plasma sample, and results showed that the acceptable relative standard deviation (4.25%) and relative recovery (99.75%) values indicated that the developed method can be used for Δ^9-THC determination level in clinical samples.

1. INTRODUCTION

Cannabinoids appear to have anti-inflammatory, neuroprotective, analgesic, anxiolytic, and pain-relieving properties, suggesting that they could be used as potential recovery mediators in athletes during regular training and competition [1, 2]. Athletes have been reported to use cannabis for anxiety

and stress relief, as well as possibly to reduce muscle spasms, and it has been proposed that athletes were primarily motivated to use cannabis because of its effects on relaxation and well-being, promoting better sleep [3-5]. As a result, cannabinoids are on the International Olympic Committee's list of prohibited drugs [6, 7]. The World Anti-Doping Agency forbids the use of any cannabinoids, natural or synthetic, during competition [8-10].

Δ^9-tetrahydrocannabinol (Δ^9-THC), better known as THC is the chemical that causes the majority of marijuana's psychological effects [11]. Δ^9-THC is the psychoactive substance responsible for the "high" associated with marijuana use, and it can also cause central nervous system depression [12, 13]. According to the National Institute on Drug Abuse, it functions similarly to cannabinoid chemicals produced naturally by the body (NIDA). Δ^9-THC is used to treat loss of appetite that causes weight loss in people with AIDS [14, 15]. Δ^9-THC is employed to cure severe nausea and vomiting induced by chemotherapy for cancer [16]. Δ^9-THC stimulates neurons involved in pleasure, memory, and cognition. THC's potential health benefits include pain relief and sleep aid, as well as relaxation, decreased anxiety, increased appetite, feelings of happiness or exhilaration, heightened imagination, and improved sensory perception. Δ^9-THC can acutely induce psychotic symptoms and impair episodic and working memory [17-19].

As a result, identifying and determining the level of Δ^9-THC in pharmaceutical compounds, body fluids, and tissues is an important criterion, and many studies have been conducted to determine the concentration of Δ^9-THC using high performance liquid chromatography [20-23], gas chromatography–mass spectrometry [24], liquid chromatography-mass spectrometry [25], fluorescence quenching method [26], MicroNIR–chemometric platform [27] and electrochemical techniques [28-35]. Among these methods, electrochemical sensors based on molecular imprinting polymers (MIPs) demonstrated good stability, a simple and low-cost fabrication method, and high selectivity in biological sample matrices containing a high number of interference species. MIPs have cavities with specific spaces that are expected to mimic the exact grooves of the template and act as a recognize center for target molecules that have the same or similar properties as the template molecules [36, 37]. Furthermore, the use of nanostructures with high conductivity and a large surface area, such as CNTs, can provide more recognition sites on the surface and facilitate electron transfer kinetics [38-40]. As a result, the purpose of this research was to develop a molecular imprinting-based sensor based on MWCNTs modified electrodes for the selective determination of Δ^9-THC as a doping agent in athlete biological fluid samples.

2. EXPERIMENT

2.1. Fabrication of modified electrodes

In an electrochemical cell with a working electrode, an auxiliary electrode (Pt plate), and a reference electrode (Ag/AgCl), MWCNTs nanostructures were electrodeposited on the surface of a screen printed carbon electrode (SPCE). The electrochemical deposition was performed at a fixed potential of -1.0 V in 0.1 M KCl (99.0%) solution with 1 mg/mL dispersed MWCNTs (95%) for 400s [41]. For preparation of the MIP-based sensor, the electropolymerization technique was used in the

potential range from 0.15 to 1.35 V at a scan rate of 50 mV/s for 20 cycles on the MWCNTs/SPCE surface through the CV in the potential range from 0.0 to 1.0 V at a scan rate of 50 mV/s for 5 cycles [42]. The electrolyte was contained 1.4 mM of methacrylic acid (99.0%, Sigma-Aldrich) as functional monomer, 0.4 mM of Δ9-THC (Sigma-Aldrich) as template molecule and 7 mM of ethylene glycol dimethylacrylate (95%, Sigma-Aldrich) as cross-linking monomer dissolved in 1 mL of methanol ($\geq$ 99.9 %, Merck Millipore, Germany), and added in 5 mL of 0.1 M PBS [43]. After electropolymerization, the electrode was immersed in ethanol solution (5% v/v) for the removal of target molecules (Δ^9- THC). Finally, the electrode was rinsed with deionized water and dried at room temperature.

2.2. Instrument and characterization methods

On an SEC1106 electrochemical workstation, cyclic voltammetry (CV) and differential pulse voltammetry (DPV) measurements were performed in 0.1M phosphate buffer solution (PBS) electrolyte (pH 7.0) electrolyte prepared from a mixture of 0.1M Na_2HPO_4 (99%, Merck Millipore, Germany). X-ray diffraction (XRD; Rigaku MiniFlex 600X radio diffractometer, Japan) and scanning electron microscopy (SEM; LEO 1525, Carl Zeiss, Oberkochen, Germany) were used to investigate the structural and morphological properties of nanostructured electrodes.

## 2.3. Preparation of the actual sample from the blood plasma of a cyclist

MIP/MWCNTs/SPCE as a sensing system for Δ^9-THC analysis in real samples were investigated using samples of cyclists' blood plasma. The cyclist was given Dronabinol 10 mg capsules (10 mg Danazol). The initial half-life is approximately 4 hours, while the terminal half-life is approximately 25-36 hours. Thus, blood plasma samples were collected 4 hours after taking Dronabinol. The blood plasma samples were centrifuged for 10 minutes at 1500 rpm, filtered, and then used to prepare 0.1 M PBS. Finally, 0.1 M PBS prepared from blood plasma samples was used as an electrochemical electrolyte. The Δ^9-THC Quantitative ELISA technique was also used to determine the concentration of Δ^9-THC in human blood plasma.

3. RESULTS AND DISCUSSION

3.1. SEM and XRD studies

Figure 1 shows SEM images of MWCNTs/SPCE and MIP/MWCNTs/SPCE. Figure 1a shows a SEM image of MWCNTs/SPCE that shows 1D nanostructures of MWCNTs with an average diameter of 45 nm and small bundles electrodeposited on the SPCE surface, resulting in a nest-like structure with a large surface area and high porosity. In the SEM image of Figure 1b, the porous thin polymeric film with polymer webbing morphology is formed onto the electrode surface for MIP/MWCNTs/SPCE, and MIP nanoscale particles can scatter on the entire surface of the MWCNTs/SPCE. The average diameter of MIP/MWCNTs on SPCE is 60 nm, and the surface of

MIP/MWCNTs/SPCE is rougher than MWCNTs/SPCE, indicating that MWCNTs are covered by a thin layer of MIP particles without changing the morphology of MWCNTs [44, 45].
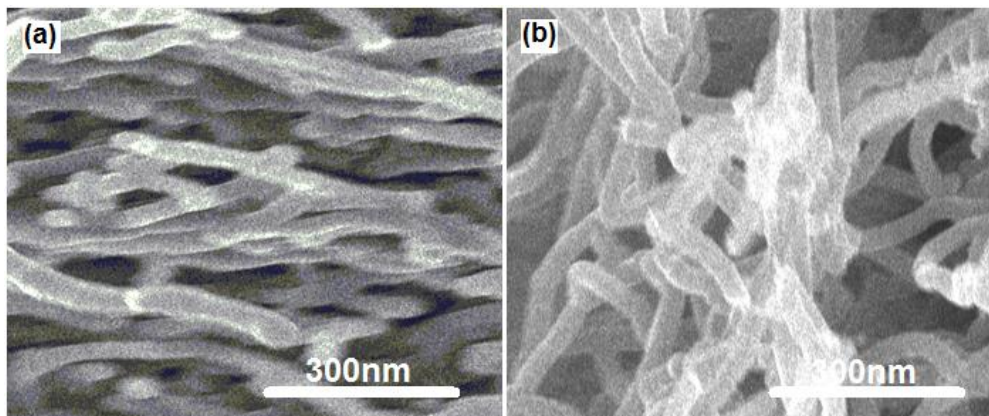
**Figure 1**. SEM images of (a) MWCNTs/SPCE and (b) MIP/MWCNTs/SPCE.

Figure 2 depicts XRD patterns of MIP, MWCNTs, and MIP/MWCNTs deposited powder. MWCNTs and MIP/MWCNTs XRD patterns show strong diffraction peaks at 25.3°, 43.7°, 51.0°, 72.75°, and 67.31°, which correspond to the (002), (101), (004), and (110) planes of MWCNTs with hexagonal graphite structure (JCPDS card no. 41-1487) [46-48], respectively. As can be seen, the intensities of diffraction peaks in MIP/MWCNTs are smaller than those found in MWCNTs, and the XRD pattern of MIP does not display any apparent diffraction peak, implying that MIP electropolymerized effectively on MWCNTs [49].
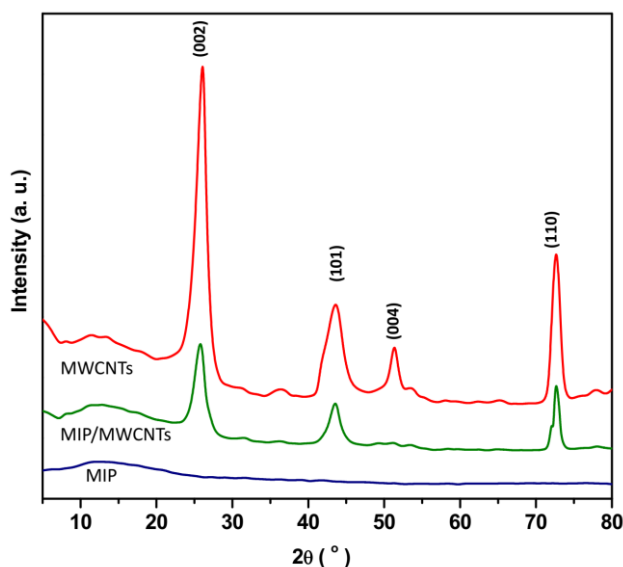

Figure 2. XRD pattern of the deposited powder of MIP, MWCNTs and MIP/MWCNTs.

3.2. Electrochemical studies

Figure 3 depicts the CV curves of SPCE, MWCNTs/SPCE and MIP/MWCNTs/SPCE in 0.1 M PBS pH 7 at a scan rate of 30 mV/s at the potential between 0.10 and 0.80 V. The CV curves were recorded in 0.1 M PBS with and without of Δ^9-THC solution. For the electrolyte solution without Δ^9-THC, as seen, the CV curves of all electrodes do not present any redox peak. After adding the 300 ng/mL of Δ^9-THC solution in electrochemical cell, the well-defined peaks at 0.51 , 0.50 and 0.47 V are appeared in CV curves of SPCE and MWCNTs/SPCE and MIP/MWCNTs/SPCE, respectively that it may be related to the anodic oxidation of Δ^9-THC through deprotonation hydroxyl group attached to C-1 mechanism and formation phenoxide anion which followed by oxidation and creation of a phenoxy radical as shown in Figure 4 [33, 50, 51]. Furthermore, MIP/MWCNTs/SPCE peak currents are observed at a lower potential with higher current intensity than SPCE and MWCNTs/SPCE. It demonstrates a significant increase in the electrocatalytic activity of MIP/MWCNTs nanostructures due to a synergistic effect between MWCNTs nanostructures and MIP molecules [52-54]. MIPs are biomimetic materials with the specific purpose of recognizing target molecules. The shaped complex between functional monomers and template molecules would provide analogues with related analyte structure during the electropolymerization procedure, and reduction of the embedded template molecules induces the memory cavities within the polymer matrix to regrow with homogeneous binding sites, imbuing the polymer with high selectivity [55, 56]. The large surface area of MIP/MWCNTs nanohybrids, combined with MWCNTs' excellent electrical conductivity, provides a direct channel for electron transfer from the recognition cavities to the electrode surface, improving the response signal [57, 58]. Electroolymerization of MIPs on MWCNTs improves the proximity of the imprinted sites to the material surfaces, facilitating electron transfer kinetics and increasing specificity and sensitivity [52, 59]. As a result, MIP/MWCNTs/SPCE were used in subsequent electrochemical studies.
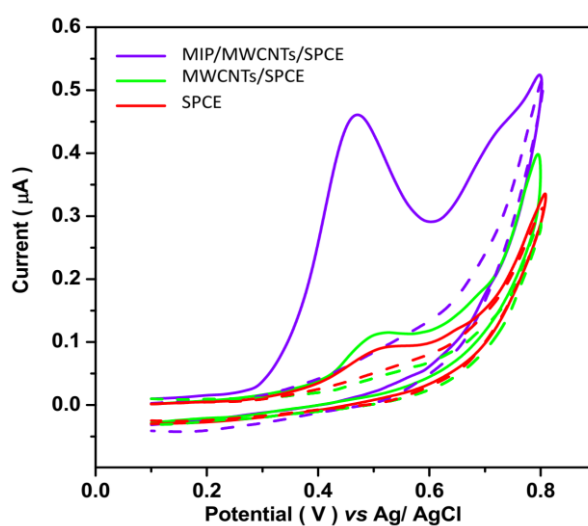

Figure 3. CV curves of SPCE, MWCNTs/SPCE and MIP/MWCNTs/SPCE in 0.1 M PBS pH 7 with and without of 300 ng/mL of Δ^9-THC solution by a scan rate of 30 mV/s at the potential between 0.10 and 0.80 V.
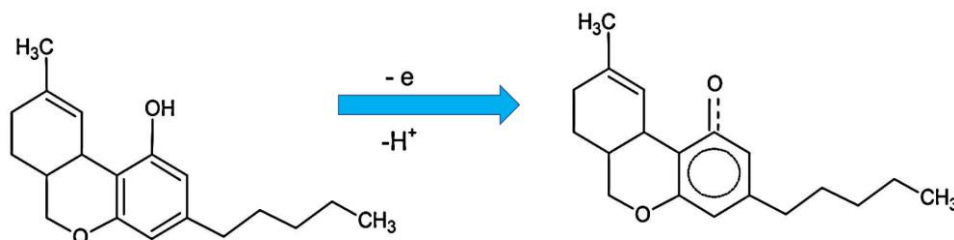
Figure 4. Mechanism of oxidation of Δ^9-THC [33].

Figure 5 shows the results of DPV measurements of MIP/MWCNTs/SPCE under consecutive injections of a solution containing 150 ng/mL Δ^9-THC solution in 0.1 M PBS pH 7 electrolyte solution at an applied potential between 0.18 and 0.72 V with a scan rate of 30 mV/s. Results reveal that the DPV peak current is linearly increased by increasing the Δ^9-THC concentration in an electrochemical cell. The calibration plot in the inset of Figure 5 demonstrates that the minimal detectable limit for Δ^9-THC is 0.37 ng/mL (S/N=3), the sensitivity of MIP/MWCNTs/SPCE THC is obtained at 0.00155 µA/ng.mL^{-1}, and linearity is over a concentration range of 0–3150 ng/mL with correlation coefficients of the standard curves > 0.99. Table 1 shows the performance of the proposed method and some of the previously reported Δ^9-THC sensors in liertures. As can be seen, MIP/MWCNTs/SPCE exhibit superior or comparable electrocatalytic performance to previously reported Δ^9-THC sensors because MWCNTs in MIP/MWCNTs nanohybrids behave as electronic bridges to enhance electron transfer among complex MIP films [60, 61]. Electroolymerization of MIP nanoparticles on MWCNTs indicates great specific surface area, and provides extremely abundant imprinting sites [60, 62].
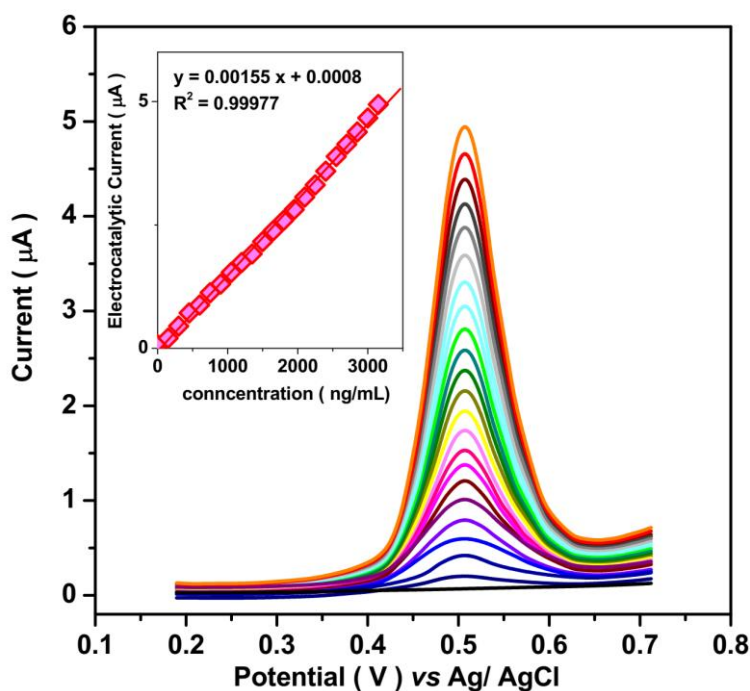
Figure 5. The results of DPV measurements of MIP/MWCNTs/SPCE under consecutive injections of a solution containing 150 ng/mL Δ^9-THC solution in 0.1 M PBS pH 7 electrolyte solution at an applied potential between 0.18 and 0.72 V with a scan rate of 30 mV/s

Table 1. The performance of electrochemical sensor for determination of Δ^9- THC in present work and released outcomes of Δ^9-THC sensors in litieretures.

Electrode	Technique	Linear range (ng/mL)	limit of detection (ng/mL)	Ref.
MIP/MWCNTs/SPCE	DPV	0 to 3150	0.17	This work
THC infused into carbon paper electrode	Chronoamperometry	---	1.25	[28]
Disposable screen printed electrode	Chronoamperometry	0.25 to 10^{+3}	0.25	[32]
AuNPs/screen printed carbon	SWV	10^{-3} to 10^{+3}	0.007	[29]
Electrodepositied THC on carbon electrode	SWV	2 to 25	1.6	[31]
Screen Printed Electrode	CV	1257 to 6289	314	[30]
Glassy carbon electrdoe	LSV	2.4 to 11.3	0.34	[33]
C18 column	HPLC	0 to 10^{+3}	---	[20]
CN and C8 columns	HPLC	0.002 to 200	5	[21]
C18 column	HPLC	1 to 150	1	[22]
XTerra®RP18 column	HPLC	10 to 100	0.5	[23]

SWV: square wave voltammetry; LSV: linear sweep voltammetry; HPLC: high performance liquid chromatography

The selectivity of the MIP/MWCNTs/SPCE as Δ^9-THC sensors was investigated in the presence of interfering substances in biological fluids. Table 2 summarizes the obtained data from DPV measurements of MIP/MWCNTs/SPCE under consecutive injections of a solution containing 100 ng/mL Δ^9-THC and 500 ng/mL interfering substances solutions in a 0.1 M PBS pH 7 electrolyte solution at an applied potential between 0.18 and 0.72 V with a scan rate of 30 mV/s. Results in Table 2 show that a considerable electrocatalytic peak current is formed after the addition Δ^9-THC solution in an electrochemical cell, and no detectable electrocatalytic responses are observed for the addition of interfering substances. The result reveals that the MIP/MWCNTs/SPCE can be great specific sensor for the determination Δ^9-THC in biological fluid samples.

The applicability and validity of MIP/MWCNTs/SPCE was investigated for determination level of Δ^9-THC in cyclist's blood plasma sample. Figure 6 and Table 2 exhibit the obtained data from DPV measurements of MIP/MWCNTs/SPCE under consecutive injections of a solution containing 50 ng/mL Δ^9-THC solutions in 0.1 M PBS pH 7 electrolyte solution prepared from cyclist's blood plasma sample at an applied potential between 0.18 and 0.72 V with a scan rate of 30 mV/s and determination results by Δ^9-THC Quantitative ELISA analyses which demonstrated the average level of Δ^9-THC in the cyclists' blood plasma sample are 1.84 ng/mL and 1.95 ng/mL by a DPV measurements and ELISA analysis, respectively, illustrating the great agreement and validity between electrochemical and ELISA analyses. Additionally, the findings of analytical studies obtained from DPV analysis by standard addition method are exhibited in Table 2. As seen, the acceptable relative standard deviation

($\geq 4.25\%$) and relative recovery ($\geq 99.75\%$) values indicated the developed method can be utilized for determining the level of Δ^9-THC in clinical samples.

Table 2. The obtained data from DPV measurements of MIP/MWCNTs/SPCE under consecutive injections of a solution containing 100 ng/mL Δ^9-THC and 500 ng/mL interfering substances solutions in in 0.1 M PBS pH 7 electrolyte solution at applied potential between 0.18 and 0.72 V with scan rate of 30 mV/s.

Substance	Added (ng/mL)	DPV peak current (µA) at 0.47 V	RSD
Δ^9-THC	100	0.1553	±0.0024
11-nor-9-carboxy-Δ^9-tetrahydrocannabinol	500	0.0339	±0.0021
11-Hydroxy-Δ^9-tetrahydrocannabinol	500	0.0227	±0.0017
Norepinephrine	500	0.0346	±0.0014
6-acetylmorphine	500	0.0262	±0.0012
Stanozolol	500	0.0333	±0.0012
Ascorbic acid	500	0.0250	±0.0015
Hydrocodone	500	0.0152	±0.0017
Buprenorphine	500	0.0225	±0.0018
Serotonin	500	0.0309	±0.0013
Dopamine	500	0.0222	±0.0011
Norbuprenorphine	500	0.0211	±0.0014
Ethylmorphine	500	0.0122	±0.0015
Acetaminophen	500	0.0175	±0.0012
Uric acid	500	0.0129	±0.0011
Amphetamine	500	0.0128	±0.0010
Methamphetamine	500	0.0101	±0.0011
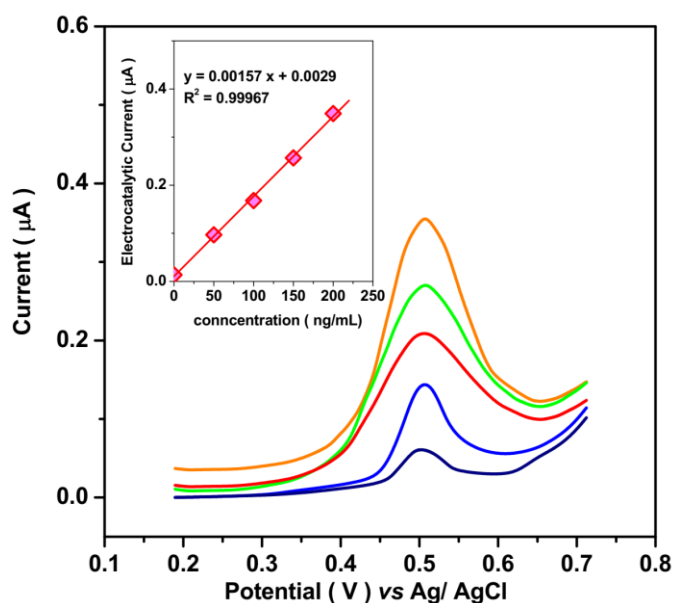
Figure 6. The results of DPV measurements of MIP/MWCNTs/SPCE under consecutive injections of a solution containing 50 ng/mL Δ^9-THC solution in 0.1 M PBS pH 7 electrolyte solution prepared from cyclist's blood plasma sample at an applied potential between 0.18 and 0.72 V with a scan rate of 30 mV/s.

Table 2. Findings of analytical studies obtained from DPV measurements and ELISA analysis for determination of Δ^9-THC in real sample prepared from cyclists's blood plasma.

DPV measurements by MIP/MWCNTs/SPCE				ELISA	
Spiked (ng/mL)	**detected (ng/mL)**	**Recovery (%)**	**RSD (%)**	**Δ^9-THC Content in cyclists's blood plasma sample (ng/mL)**	**RSD (%)**
0.00	1.84	---	3.38	1.95	3.76
50.0	51.34	99.00	3.75		
100.0	101.54	99.70	4.25		
150.0	150.74	99.26	4.05		
200.0	201.34	99.75	3.23		

4. CONCULUSION

In summary, the goal of this study was to create an electrochemical biosensor based on MIP/MWCNTs/SPCE for the selective detection of Δ^9-THC as a doping agent in athlete biological fluid samples. For MIP/MWCNTs/SPCE fabrication, MWCNTs nanostructures were electrodeposited on the SPCE, and MIP was electropolymerized on the MWCNTs/SPCE surface. SEM and XRD results confirmed that a thin layer of MIP particles covered MWCNTs without changing their morphology. Electrochemical studies revealed a significant increase in electrocatalytic activity and electivity of MIP/MWCNTs nanostructured electrodes due to the synergistic effect of MWCNTs nanostructures and MIP molecules. Results demonstrated that the minimal detectable limit for Δ^9-THC was 0.37 ng/mL (S/N=3), the sensitivity of MIP/MWCNTs/SPCE THC was obtained at 0.00155 μA/ng.mL^{-1}, and linearity was over a concentration range of 0-3150 ng/mL with correlation coefficients of the standard curves > 0.99. When the proposed method's performance was compared to that of some previously reported 9-THC sensors in the literature, it was discovered that MIP/MWCNTs/SPCE exhibited better or comparable electrocatalytic performance than previously reported Δ^9-THC sensors because the MWCNTs in MIP/MWCNTs nanohybrids act as electronic bridges to accelerate electron transfer among the complex MIP film. The applicability and validity of MIP/MWCNTs/SPCE were investigated for Δ^9-THC determination level in a cyclist's blood plasma sample, and the results demonstrated the great agreement and validity between electrochemical and ELISA analyses, as well as the acceptable relative standard deviation and relative recovery values, indicating that the developed method can be used for Δ^9-THC determination level in clinical samples.

References

1. H.M. Hashiesh, C. Sharma, S.N. Goyal, B. Sadek, N.K. Jha, J. Al Kaabi and S. Ojha, *Biomedicine & pharmacotherapy*, 140 (2021) 111639.
2. Z. Duan, C. Li, Y. Zhang, M. Yang, T. Gao, X. Liu, R. Li, Z. Said, S. Debnath and S. Sharma, *Frontiers of Mechanical Engineering*, (2022) 1.
3. M.A. Huestis, I. Mazzoni and O. Rabin, *Sports medicine*, 41 (2011) 949.
4. P. Hao, H. Li, L. Zhou, H. Sun, J. Han and Z. Zhang, *ACS sensors*, 7 (2022) 775.
5. H. Karimi-Maleh, H. Beitollahi, P.S. Kumar, S. Tajik, P.M. Jahani, F. Karimi, C. Karaman, Y.

Vasseghian, M. Baghayeri and J. Rouhi, *Food and Chemical Toxicology*, (2022) 112961.

6. M. Yang, C. Li, Y. Zhang, Y. Wang, B. Li, D. Jia, Y. Hou and R. Li, *Applied Thermal Engineering*, 126 (2017) 525.
7. J. Rouhi, C.R. Ooi, S. Mahmud and M.R. Mahmood, *Materials Letters*, 147 (2015) 34.
8. M.A. Ware, D. Jensen, A. Barrette, A. Vernec and W. Derman, *Clinical Journal of Sport Medicine*, 28 (2018) 480.
9. X. Xiao, B. Mu, G. Cao, Y. Yang and M. Wang, *Journal of Science: Advanced Materials and Devices*, 7 (2022) 100430.
10. X. Cui, C. Li, Y. Zhang, Z. Said, S. Debnath, S. Sharma, H.M. Ali, M. Yang, T. Gao and R. Li, *Journal of Manufacturing Processes*, 80 (2022) 273.
11. M. Husairi, J. Rouhi, K. Alvin, Z. Atikah, M. Rusop and S. Abdullah, *Semiconductor Science and Technology*, 29 (2014) 075015.
12. M.E. Musselman and J.P. Hampton, *Pharmacotherapy: The Journal of Human Pharmacology and Drug Therapy*, 34 (2014) 745.
13. W.-F. Lai and W.-T. Wong, *Pharmaceutics*, 13 (2021) 787.
14. A. Ejaz, H. Babar, H.M. Ali, F. Jamil, M.M. Janjua, I.R. Fattah, Z. Said and C. Li, *Sustainable Energy Technologies and Assessments*, 46 (2021) 101199.
15. C. Li, J. Li, S. Wang and Q. Zhang, *Advances in Mechanical Engineering*, 5 (2013) 986984.
16. H. Goyal, U. Singla, U. Gupta and E. May, *European journal of gastroenterology & hepatology*, 29 (2017) 135.
17. D. Luan, A. Liu, X. Wang, Y. Xie and Z. Wu, *Discrete Dynamics in Nature and Society*, 2022 (2022) 1.
18. H. Li, Y. Zhang, C. Li, Z. Zhou, X. Nie, Y. Chen, H. Cao, B. Liu, N. Zhang and Z. Said, *Korean Journal of Chemical Engineering*, 39 (2022) 1107.
19. J. Rouhi, M. Alimanesh, R. Dalvand, C.R. Ooi, S. Mahmud and M.R. Mahmood, *Ceramics International*, 40 (2014) 11193.
20. E.C. Nyoni, B.R. Sitaram and D.A. Taylor, *Journal of Chromatography B: Biomedical Sciences and Applications*, 679 (1996) 79.
21. L. Karlsson, *Journal of Chromatography B: Biomedical Sciences and Applications*, 417 (1987) 309.
22. L.K. Thompson and E.J. Cone, *Journal of Chromatography B: Biomedical Sciences and Applications*, 421 (1987) 91.
23. H. Kokubun, Y. Uezono and M. Matoba, *Gan to kagaku ryoho. Cancer & chemotherapy*, 41 (2014) 471.
24. H. Khajuria and B.P. Nayak, *Egyptian Journal of Forensic Sciences*, 4 (2014) 17.
25. H. Teixeira, P. Proença, A. Castanheira, S. Santos, M. López-Rivadulla, F. Corte-Real, E.P. Marques and D.N. Vieira, *Forensic science international*, 146 (2004) S61.
26. C. Tan, N. Gajovic-Eichelmann, W.F. Stöcklein, R. Polzius and F.F. Bier, *Analytica chimica acta*, 658 (2010) 187.
27. R. Risoluti, G. Gullifa, A. Battistini and S. Materazzi, *Analytical Chemistry*, 91 (2019) 6435.
28. M. Renaud-Young, R.M. Mayall, V. Salehi, M. Goledzinowski, F.J. Comeau, J.L. MacCallum and V.I. Birss, *Electrochimica Acta*, 307 (2019) 351.
29. S. Eissa, R.A. Almthen and M. Zourob, *Microchimica Acta*, 186 (2019) 1.
30. M.A. Balbino, I.C. Eleoterio, M.F. de Oliveira and B.R. McCord, *Sensors & Transducers*, 207 (2016) 73.
31. G.A. Ortega, S.R. Ahmed, S.K. Tuteja, S. Srinivasan and A.R. Rajabzadeh, *Talanta*, 236 (2022) 122863.
32. C. Wanklyn, D. Burton, E. Enston, C.-A. Bartlett, S. Taylor, A. Raniczkowska, M. Black and L. Murphy, *Chemistry Central Journal*, 10 (2016) 1.
33. M.A. Balbino, M.M.T. de Menezes, I.C. Eleotério, A.A. Saczk, L.L. Okumura, H.M. Tristão and M.F. de Oliveira, *Forensic Science International*, 221 (2012) 29.

34. E.R. Darzi and N.K. Garg, *Organic letters*, 22 (2020) 3951.
35. N. Naderi, M. Hashim and J. Rouhi, *International Journal of Electrochemical Science*, 7 (2012) 8481.
36. H. Setiyanto, S. Rahmadhani, S. Sukandar, V. Saraswaty, M.A. Zulfikar and N. Mufti, *International Journal of Electrochemical Science*, 15 (2020) 5477.
37. B. Liu, J. Yan, M. Wang and X. Wu, *International Journal of Electrochemical Science*, 13 (2018) 11953.
38. H. Zhang, Y. Gui, Y. Cao, M. Wang and B. Liu, *International Journal of Electrochemical Science*, 14 (2019) 11630.
39. M. Amatatongchai, W. Sroysee, P. Sodkrathok, N. Kesangam, S. Chairam and P. Jarujamrus, *Analytica chimica acta*, 1076 (2019) 64.
40. H. Li, Y. Zhang, C. Li, Z. Zhou, X. Nie, Y. Chen, H. Cao, B. Liu, N. Zhang and Z. Said, *The International Journal of Advanced Manufacturing Technology*, 120 (2022) 1.
41. Y. Liu, S. Yang and W. Niu, *Colloids and Surfaces B: Biointerfaces*, 108 (2013) 266.
42. X. Cetó, C.P. Saint, C.W. Chow, N.H. Voelcker and B. Prieto-Simón, *Sensors and Actuators B: Chemical*, 237 (2016) 613.
43. M. Nestić, S. Babić, D.M. Pavlović and D. Sutlović, *Forensic Science International*, 231 (2013) 317.
44. J. Rouhi, S. Mahmud, S.D. Hutagalung and N. Naderi, *Electronics letters*, 48 (2012) 712.
45. H. Karimi-Maleh, C. Karaman, O. Karaman, F. Karimi, Y. Vasseghian, L. Fu, M. Baghayeri, J. Rouhi, P. Senthil Kumar and P.-L. Show, *Journal of Nanostructure in Chemistry*, (2022) 1.
46. G. Zou, D. Yu, J. Lu, D. Wang, C. Jiang and Y. Qian, *Solid state communications*, 131 (2004) 749.
47. W.-F. Lai, *Molecular pharmaceutics*, 18 (2021) 1833.
48. T. Gao, C. Li, Y. Wang, X. Liu, Q. An, H.N. Li, Y. Zhang, H. Cao, B. Liu and D. Wang, *Composite Structures*, 286 (2022) 115232.
49. Y. Yang, X. Meng and Z. Xiao, *RSC advances*, 8 (2018) 9802.
50. W.-F. Lai, *Journal of Drug Delivery Science and Technology*, 59 (2020) 101916.
51. X. Wu, C. Li, Z. Zhou, X. Nie, Y. Chen, Y. Zhang, H. Cao, B. Liu, N. Zhang and Z. Said, *The International Journal of Advanced Manufacturing Technology*, 117 (2021) 2565.
52. J. Zhang, X.-T. Guo, J.-P. Zhou, G.-Z. Liu and S.-Y. Zhang, *Materials Science and Engineering: C*, 91 (2018) 696.
53. Y. Zhang, H.N. Li, C. Li, C. Huang, H.M. Ali, X. Xu, C. Mao, W. Ding, X. Cui and M. Yang, *Friction*, 10 (2022) 803.
54. J. Rouhi, S. Mahmud, S.D. Hutagalung, N. Naderi, S. Kakooei and M.J. Abdullah, *Semiconductor Science and Technology*, 27 (2012) 065001.
55. J. Zhang, X.-T. Guo, J.-P. Zhou, G.-Z. Liu and S.-Y. Zhang, *Materials Science and Engineering: C*, 91 (2018) 696.
56. L. Tang, Y. Zhang, C. Li, Z. Zhou, X. Nie, Y. Chen, H. Cao, B. Liu, N. Zhang and Z. Said, *Chinese Journal of Mechanical Engineering*, 35 (2022) 1.
57. K. Tan, Q. Ma, J. Luo, S. Xu, Y. Zhu, W. Wei, X. Liu and Y. Gu, *Biosensors and Bioelectronics*, 117 (2018) 713.
58. H. Karimi-Maleh, R. Darabi, M. Shabani-Nooshabadi, M. Baghayeri, F. Karimi, J. Rouhi, M. Alizadeh, O. Karaman, Y. Vasseghian and C. Karaman, *Food and Chemical Toxicology*, 162 (2022) 112907.
59. H. Wang, K. Wang, Q. Xue, M. Peng, L. Yin, X. Gu, H. Leng, J. Lu, H. Liu and D. Wang, *Brain*, 145 (2022) 83.
60. S. Xu, G. Lin, W. Zhao, Q. Wu, J. Luo, W. Wei, X. Liu and Y. Zhu, *ACS applied materials & interfaces*, 10 (2018) 24850.
61. W.-F. Lai, R. Tang and W.-T. Wong, *Pharmaceutics*, 12 (2020) 725.
62. S. Ren, W. Cui, Y. Liu, S. Cheng, Q. Wang, R. Feng and Z. Zheng, *Sensors and Actuators A:*

Physical, (2022) 113772